POWDER LAYER POSITION ACCURACY IN POWDER-BASED RAPID PROTOTYPING

Sang-Joon John Lee Emanuel Sachs Michael Cima

Department of Mechanical Engineering
Department of Materials Science and Engineering

Massachusetts Institute of Technology
Cambridge, Massachusetts 02139

Abstract

Layer position accuracy in powder-based processes such as Three Dimensional Printing and Selective Laser Sintering is a fundamental concern for dimensional control in the vertical direction. Ideally, each powder layer is generated at a vertical position that remains fixed at a prescribed distance from the floor of the powder bed. However, the powder bed beneath any given layer is compressible. Loads imparted to the top of that layer may cause it to displace downward. The weight of subsequent layers is an inherent source of load, that increases with the number of layers added. Other possible causes for position error include mechanical forces applied during powder spreading and powder densification from vibration.

Vertical displacements at various levels within powder beds have been measured for a set of aluminum oxide powders, using the layering process of 3D Printing. The mean displacement in a 76.2 mm deep bed ranged from 23 microns for a 30-micron platelet-shaped powder to over 260 microns for a 9-micron platelet-shaped sample. In all cases, position errors were most severe in the middle regions of the powder beds, with diminishing magnitude toward the top and bottom.

A model for layer displacement has been examined using experimental data for compressibility and applied load. Predictions made from the model captured the relative magnitudes of actual errors at various positions within layered powder beds.

Introduction

Several rapid prototyping technologies fabricate solid freeforms in a layer-by-layer sequence, with each layer representing a two-dimensional "slice" of the final part [Wohlers]. Processes known as Three Dimensional Printing [Sachs] and Selective Laser Sintering [Deckard] create the slices by joining selected areas of thin powder distributions.

Figure 1 shows the basic operating sequence of 3D Printing. Each cycle begins with fine powder, spread into a thin layer. A slicing algorithm draws detailed information for every layer, from a CAD representation of the desired part, Then a raster-scanning printhead (using a technology similar to ink-jet printing) selectively applies a binder material to join particles where the object is to be formed. A piston that supports the powder bed lowers so that the next powder layer can be leveled and selectively joined. The layered building cycle repeats until the part is completed. After a heat treatment, removal of the unbound powder reveals the finsihed part.

Figure 1. Three Dimensional Printing Process

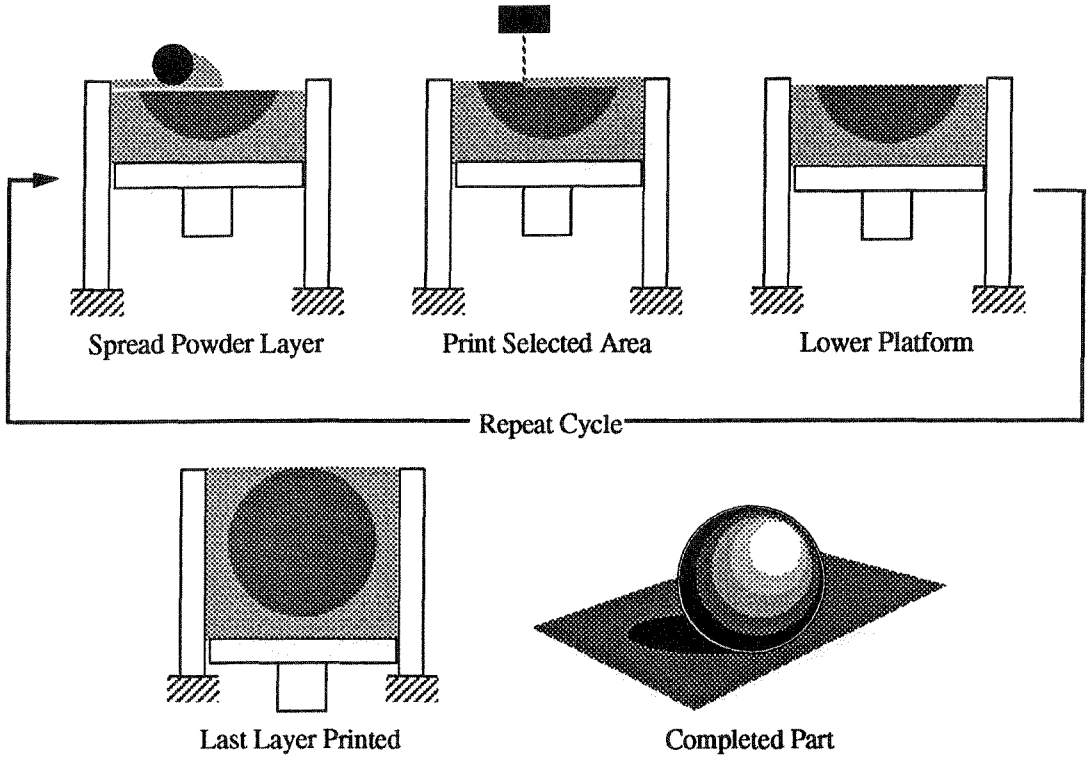

The stability of dry-powder layer positions may be critical to dimensional accuracy in the vertical direction. Loads applied from above each layer, combined with the inherent compressibility of the powder bed below, may cause a layer to deviate from its original position (with respect to the powder bed floor). The vertical position of a layer is relatively secure within the bulk region of a part, because the particles above and below it are bound in place. However, a delicate or weakly-supported feature may suffer a change in position if the powder beneath it compresses when loaded from above. Figure 2 shows an example in which the vertical spacing between two regions of a part may be inaccurate because the powder beneath each of them compresses by different amounts.

Figure 2. Example of the Significance of Powder Layer Position Accuracy

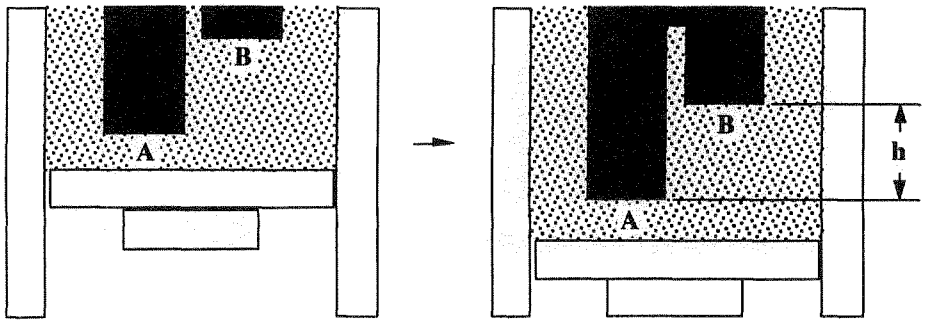

The experiments described in this paper uses the 3DP layering process to study some examples of powder layer displacement, and to develop a basic understanding of the interaction between load and compressibility. *Dry* conditions are examined as a worst-case scenario for layer displacement, presuming that layers mutually supported by binder are less prone to changing position. Although particle morphology is not studied formally, four samples of aluminum oxide are used to roughly compare particles that differ in size and shape.

Figure 3 details the steps of the 3D Printing layering sequence. Each complete cycle involves two passes over the powder bed. In the first pass, a bead of powder is spread into a uniform distribution, while applying counter-rotation and vibration. The rotation enhances particle flow, while the vibration increases packing density and breaks agglomerates. The second pass strikes a clean surface onto which binder may be printed. Rotation and vibration of the spreading device are made possible by the configuration shown in Figure 4.

Figure 4. Powder Layering Sequence for 3D Printing (Side View)

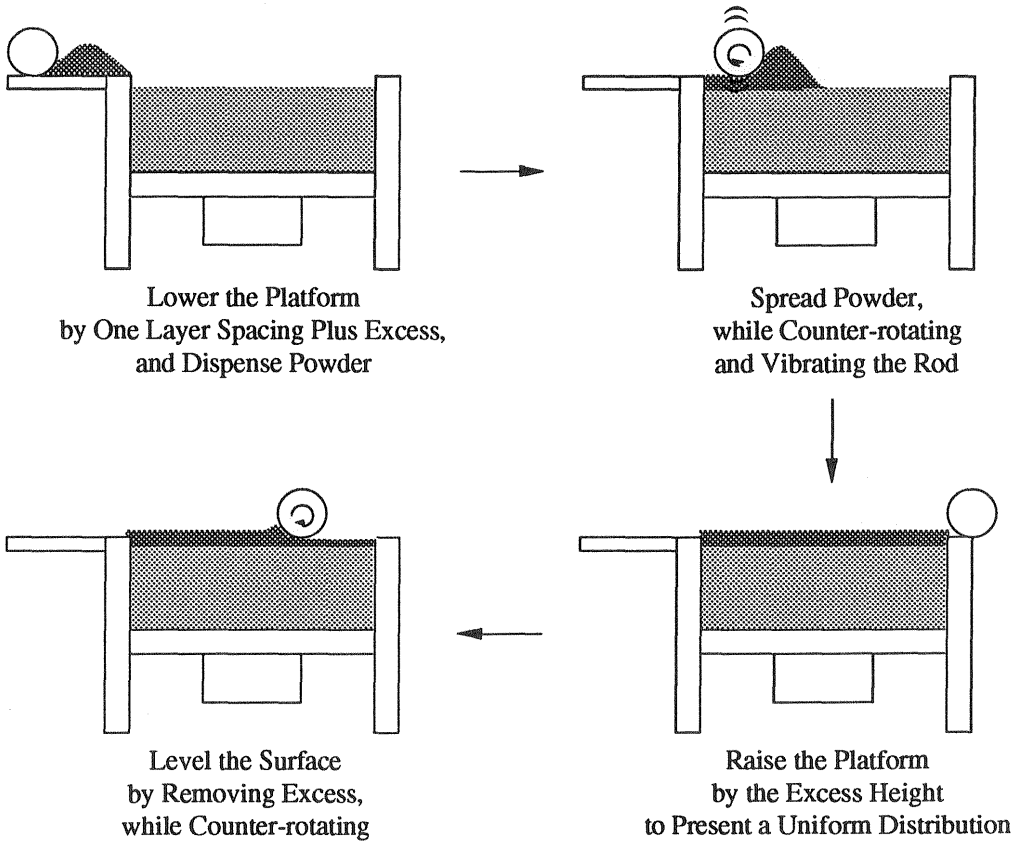

Figure 4. Powder Spreading Apparatus (Front View)

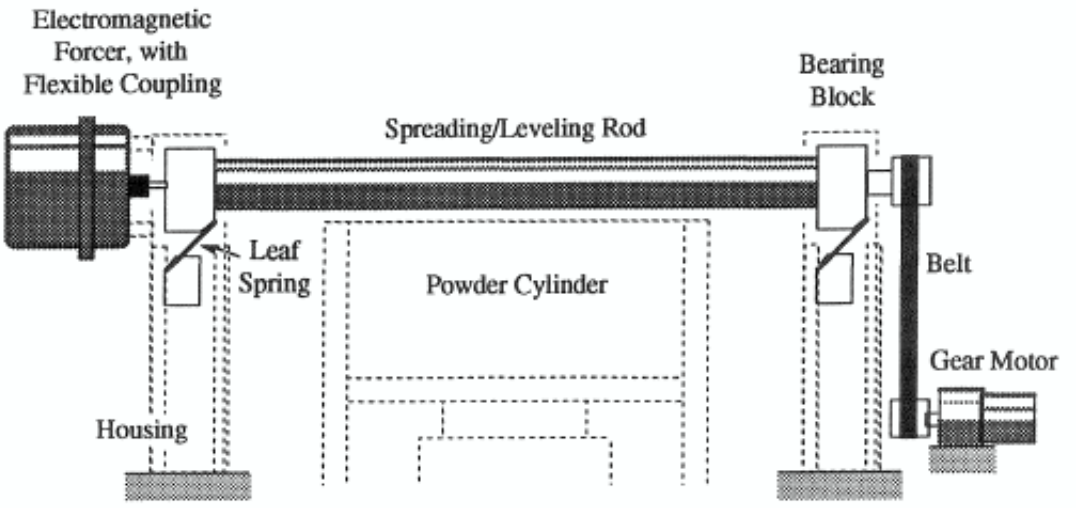

Before beginning layer position measurements, operating conditions that favor high packing density were studied by performing a designed experiment. A description of the factorial design is provided as an appendix. High packing density at every layer is desirable for minimizing compressibility [Fayed] and reducing compaction from incidental vibration.

Layer Displacement Measurements

A powder bed that is not fully dense will compress to some degree when loaded from above. Consequently, the vertical position of layers within the bed will displace downward. To measure the magnitude of this effect, graphite needles were placed at selected positions during experimental layering runs. As layers were added, the needles moved with the powder particles and thereby marked the change in layer position (see Figure 5). After completion of all layers, incremental search passes with a scraper blade would locate the altered positions of the markers.

Figure 5. Layer Displacement Measurement

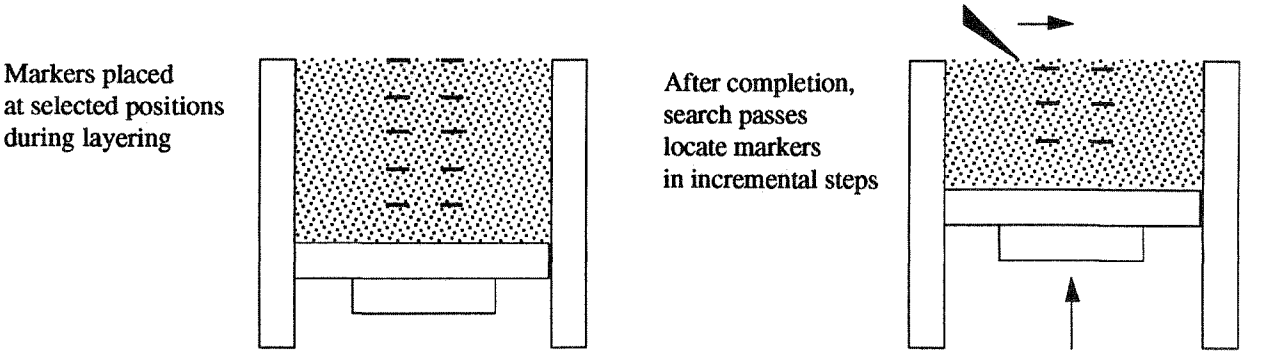

The experiments were conducted in a bed 76.2 mm deep, with a 90 mm x 90 mm cross-sectional area. Layers were spaced 190.5 microns apart. The spreader was traversed at 50 mm/s, with a counter-rotation speed of 75 mm/s on the outer diameter of the rod. Vibration was applied at 250 Hz with 50-micron peak-to-peak amplitude. Alumina powder was used in two sizes (about 10 and 30 microns, typical diameter) and two shapes (platelet-shaped or spherical).

Marker trace experiments generated the results shown in Figure 6. The plots are oriented such that the bottom of each plot corresponds to the bottom of the powder bed, and the magnitude of the bars correspond to the amount of *downward* displacement for each of the measured layers.

Figure 6. Measured Errors in Layer Position

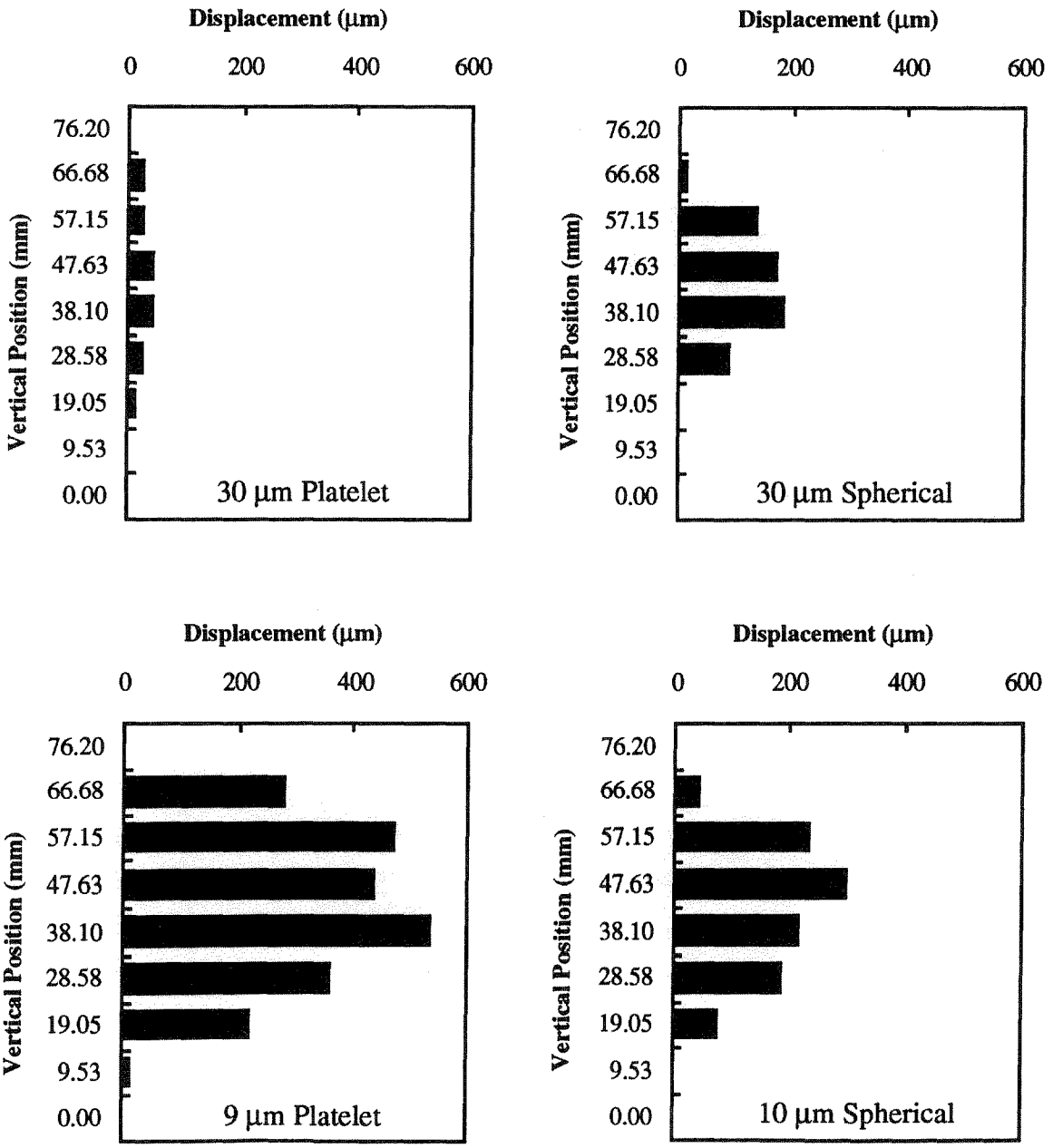

Each of the powder samples exhibited the greatest displacement in the middle region of the bed. Smaller displacement error was observed near the top and bottom. The error profiles can be interpreted as resulting from the combined effect of load and compressibility. The layers near the bottom have significant weight above, but show little error because they are near the floor of a rigid platform. Although the layers near the top have much material to compress below, they also have small error magnitudes because there is very little load from above. In contrast, the middle layers have the greatest error magnitudes because they have substantial loading from above, and a sufficient quantity of powder to compress below.

Experiments were conducted to examine load and compressibility more closely. Measurements for load and compressibility were then combined to generate error predictions. Comparison of the predictions with actual displacement measurements provides a means of understanding the mechanics that affect vertical position accuracy in powder-based processes.

Compressibilities Of Powder Beds

A powder bed is an assembly of a large number of particles with a significant fraction of void space. A bed of powder will exhibit some compression under load [Dallavalle], even at relatively high packing density. The apparatus shown in Figure 7 was used to make compressibility measurements. An opaque mask was attached to a thin latex membrane, which in turn covered a small pressure chamber. When pressure was applied to the chamber, the membrane and mask moved downward with the top surface of the powder. A (stationary) solar cell was calibrated to measure displacement as the mask exposed more light. Pressure was applied from zero to 1250 Pa (1250 Pa simulates the weight of a typical full powder bed), onto a 50-layer powder bed (at 190.5 micron layer thickness). The membrane was chosen over a rigid platform because its compliance more closely simulates the movement of a powder layer.

Figure 7. Compressibility Measurement Apparatus

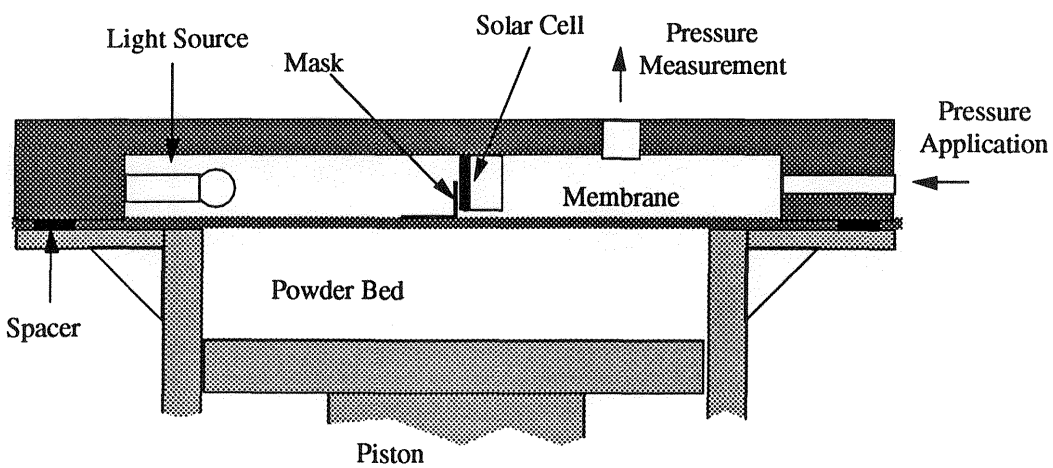

Figure 8 presents the compressibility data for the four powders, tested in a bed of 190.5 μm layers, stacked 9.525 mm deep. Compressibility is expressed in strain vs. stress, where the strain is the displacement divided by the stack height and the stress is the pressure applied to the top surface.

Figure 8. Compressibility Data

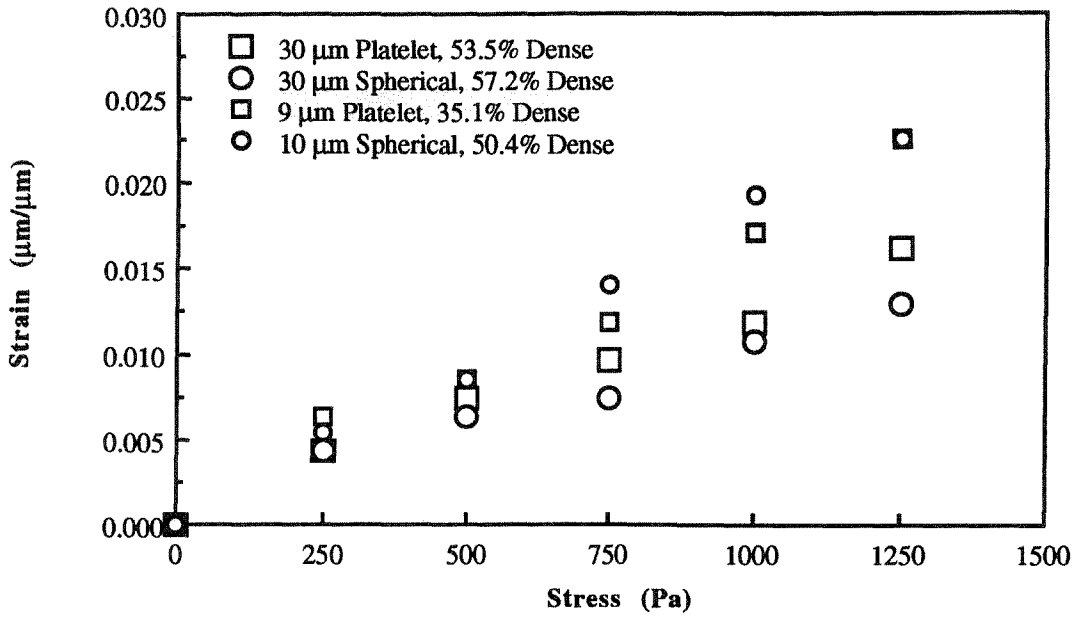

In this paper, compressibility is interpreted as the slope of a fitted line through the strain-stress data. High compressibility means that a powder bed will have a large change in height for a given load. The compressibilities of the sample powders are:

Large Platelet	1.15×10^{-4}	Pa^{-1}
Large Spherical	9.30×10^{-5}	Pa^{-1}
Small Platelet	1.62×10^{-4}	Pa^{-1}
Small Spherical	1.75×10^{-4}	Pa^{-1}

Expressing measurements in terms of strain presumes that the compression of a bed scales linearly with stack height. That is, for a given load, a stack twice as high as another will compress twice as much. This assumption should be valid as long as the powder does not approach tap density. However, when load is applied in large increments, the combination of wall friction and extensive inter-particle bridging may reduce the compression of taller beds. Therefore, the relatively shallow 9.525 mm stack height was used in these measurements. In the actual layering process, small load increments (typically 5 Pa) and vibration during spreading minimize non-linearity caused by wall friction and inter-particle bridging.

Now having a measure of how a powder bed responds to load, the loads are measured in the following set of experiments.

Loads Applied To Powder Layers

Each layer within a powder bed will be subjected to vertical loading. An inherent source of load is the weight of subsequent powder layers. A secondary compressive load may arrise if a significant quantity of powder is trapped under the spreader rod as it traverses the powder surface. The weight can be calculated easily from packing density and volume, but a special technique was required to check the significance of loads during actual spreading.

A pressure sensor was designed to measure the force exerted on a powder bed during traversal of the spreader rod. As Figure 9 shows, a shallow pocket connected to a silicon pressure transducer was imbedded into the piston floor. The pocket was covered with a thin latex membrane and filled with oil to act as a load sensor. The pocket was oriented such that its signal would show a peak if the spreader rod caused a significant pressure increase as it passed over the bed.

Figure 9. Powder Bed Load Measurement Device

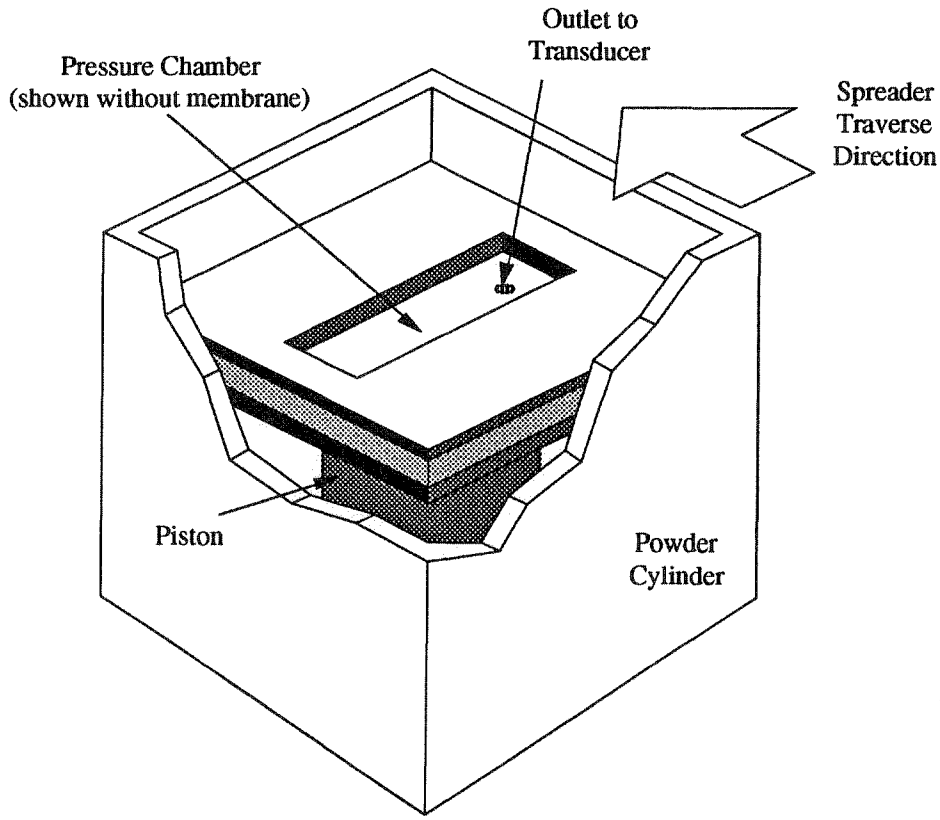

No significant pressure increase could be detected as the spreader rod traversed over the powder bed under a wide range of conditions. Traverse speeds were varied between 20 mm/s and 100 mm/s and rotation speeds varied between 20 mm/s and 100 mm/s on the circumference . Bed depths as shallow as 1 mm and as deep as 67 mm were examined. Figure 10 shows typical real-time pressure measurements as the spreader rod makes one back-and-forth traverse across a bed of 10-micron spherical alumina.

Figure 10. Pressure Measurements during Spreader Traverse

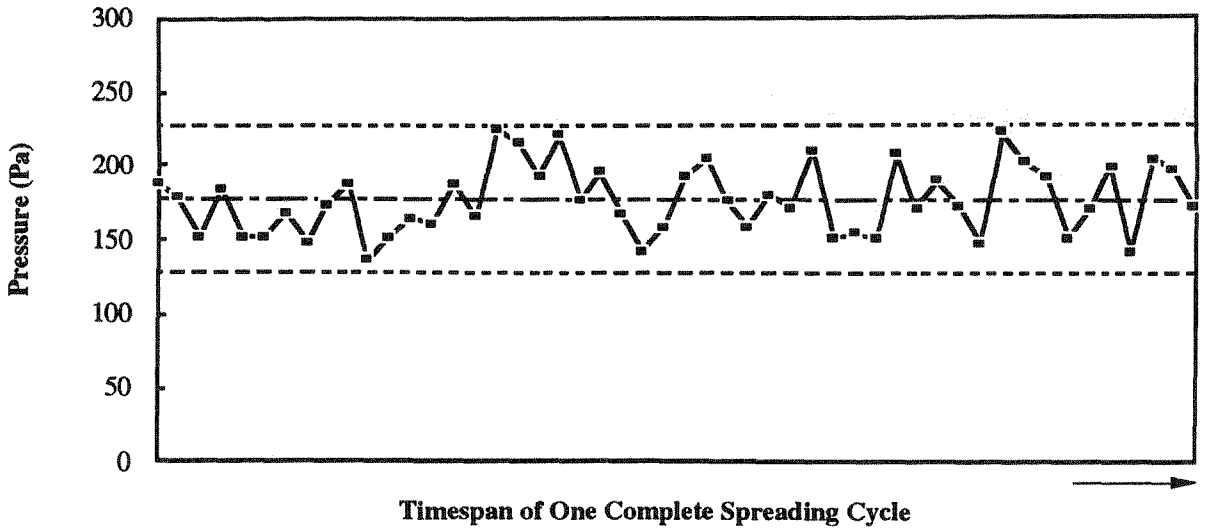

A standard deviation was computed from long runs of data while the spreader was at rest. Upper and lower limits are set at 3 standard deviations from the mean. If the spreader rod increased pressure significantly, the plots would show two peaks (for each of the pass over the bed). The results suggest that the dominant source of load upon a given layer is simply the weight of subsequent layers.

Error Predictions

Displacement predictions for a layer can be made using the compressibility of the powder by assuming the static weight of layers above is the primary source of load. Compressibility from experimental data and load computed from density and volume lead to the following key relationships for a prediction of layer displacement:

$$\text{Compressibility} = \frac{\text{Strain}}{\text{Stress}} \qquad \text{Strain} = \frac{\text{Displacement}}{\text{Vertical Position}} \qquad \text{Stress} = \frac{\text{Load}}{\text{Interface Area}}$$

$$\text{Load} = \text{Density} \cdot (\text{Total Height} - \text{Vertical Position}) \cdot \text{Interface Area}$$

Letting C = Compressibility, ρ = Density, and H = Total Height, layer displacement Δy is shown to be a quadratic function of vertical position (y) from the bed floor:

$$\Delta y = (\rho\, C\, H)\, y - (\rho\, C)\, y^2$$

Figure 11 shows the layer displacement predictions for the four powder samples, superimposed upon the error traces from direct measurement.

Figure 11. Layer Displacement Predictions

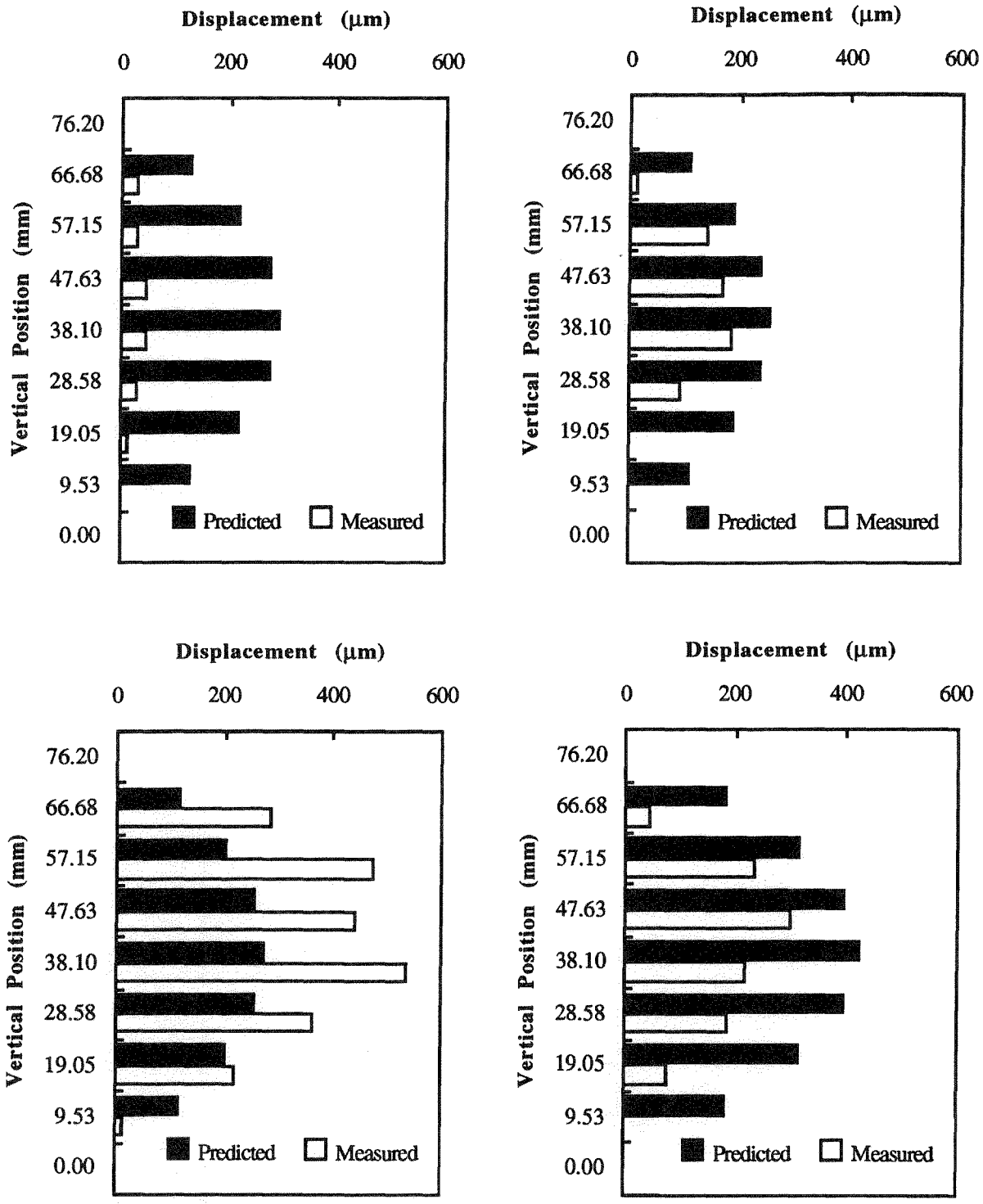

The results show that the compressibility and load data indeed capture the quadratic shape of the measured error profiles. The spherical powder samples also showed close agreement between predicted and measured magnitudes. The platelet-shaped particles showed less predictability with respect to magnitudes.

The over-estimation for the large disk-shaped powder may be the result of wall friction and internal bridging of particles. Figure 12 compares expected weight versus the weight measured using the pressure sensor. The measurements show that the full load of the powder stack is always slightly less than the expected load. The largest deviation was experienced by the 30-micron platelet powder, which also exhibited the largest discrepancy between measured and predicted vertical displacement.

Figure 12. Actual Transmitted Load versus Expected Weight

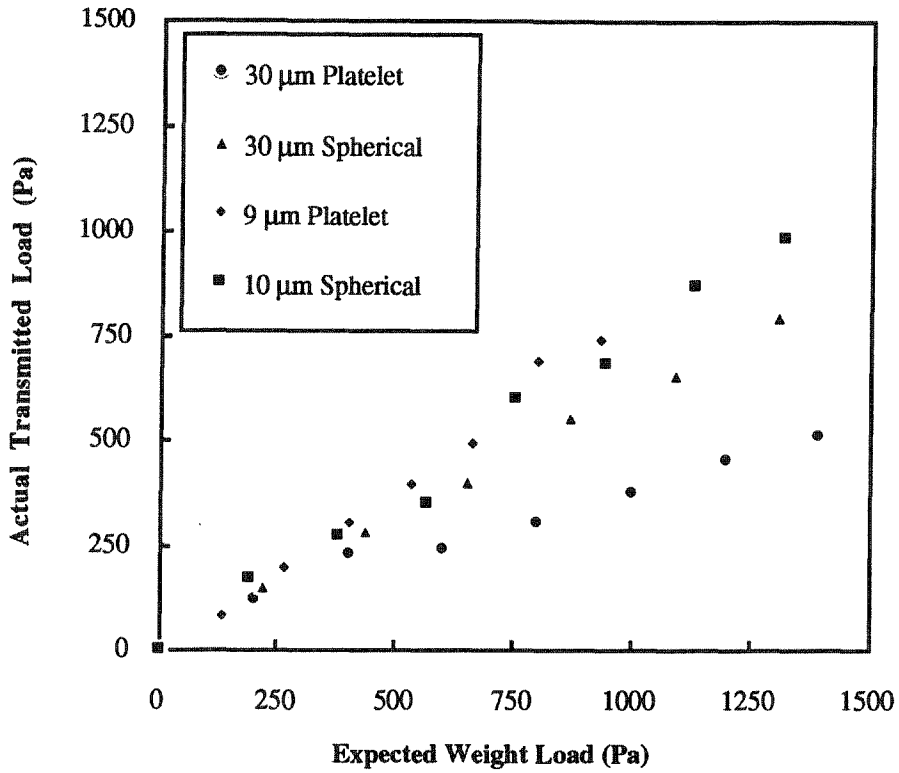

Conclusions

The following conclusions can be made based on measured layer displacements and experiments on compressibility and load: (1) Layer displacements in a dry powder bed may have significant magnitude compared with layer spacing. (2) Layer displacements have a characteristic parabolic profile, with greatest errors for middle layers and diminishing magnitude for top-most and bottom-most layers. (3) The weight of subsequent powder appears to be the dominant source of load on any given powder layer. (4) Predictions based on weight and compressibility make fair approximations to actual errors in layer position. (5) Results are highly material-dependent. Particle geometry and packing density affect the magnitudes of errors. (6) In some cases, wall friction may significantly reduce the powder weight that is transmitted to lower layers.

A suggestion for accuracy improvement is the investigation of techniques that help to fix particles in place. Procedures such as misting with water or a temporary chemical agent could reduce compressibility and thereby reduce layer displacements.

Acknowledgements

NSF Strategic Manufacturing Initiative
MIT Leaders for Manufacturing
ARPA
Three Dimensional Printing Consortium
- 3M
- AMP
- Ashland Chemical
- Boeing
- E-Systems
- Hasbro
- Howmet
- Johnson & Johnson
- National Center for Manufacturing Sciences
- Procter & Gamble
- Sandia National Labs
- United Technologies

References

Brown, R. L. & Richards, J. C., *Principles of Powder Mechanics*, Pergamon Press, Oxford, 1970.

Dallavalle, J. M., *Micrometrics: The Technology of Fine Particles*, 2nd ed., Pitman Publishing Corporation, New York, 1948.

Deckard, C. & Beaman, J., "Recent Advances in Selective Laser Sintering," *Fourteenth Conference on Production Research and Technology*, University of Michigan, Oct. 1987, pp. 447-452.

Fayed, M. E. & Otten, L., eds., *Handbook of Powder Science and Technology*, Van Nostrand Reinhold Company, New York, 1984.

Iinoya, K., Gotoh, K., Higashitani, K., eds., *Powder Technology Handbook*, Marcel Decker, Inc., New York, 1991.

Sachs, E., Cima, M., Williams, P., Brancazio, D, and Cornie, J., "Three Dimensional Printing: Rapid Tooling and Prototypes Directly From a CAD Model," accepted for publication in the *Journal of Engineering for Industry*, 1990, p. 13.

Wohlers, T., "Creating Parts by Layers", *Cadence*, April 1989, pp. 73-76.

Appendix: Designed Experiment to Maximize Packing Density

Experimental design has been implemented to characterize the powder layering process in terms of how input parameters affect layered packing density.To address many factors in a reasonable number of experiments, only two levels (low and high) were examined for each control variable. A 1/8 fractional design (2^{7-3}) [Montgomery: *Statistical Quality Control*] is used to reduce the number of experiments to a reasonable number. The parameters in Table A1 were selected as control variables to understand the conditions affecting layered packing density.

Table A1. Layered Packing Density Control Variables

Variable	Symbol	Low	High	Units
Layer Spacing	S	127	254	μm
Traverse Speed	T	50	100	mm/s
Rotation Speed	R	1.5	2.0	rev/s
Vibration Frequency	F	125	400	Hz
Vibration Amplitude	A	25	50	μm zero-to-peak
Moisture Exposure	M	35	80	% sat @ 25 °C
Spreading Excess	E	31.75	127	μm

The 2^{7-3} experimental array for a given powder is shown in Table A2, with (-1) representing low levels and (+1) representing high levels of the control variables.

Table A2. 2^{7-3} Fractional Factorial Design

Run	S	T	R	M	F	A	E
1	-1	-1	-1	-1	-1	-1	-1
2	+1	-1	-1	-1	+1	-1	+1
3	-1	+1	-1	-1	+1	+1	-1
4	+1	+1	-1	-1	-1	+1	+1
5	-1	-1	+1	-1	+1	+1	+1
6	+1	-1	+1	-1	-1	+1	-1
7	-1	+1	+1	-1	-1	-1	+1
8	+1	+1	+1	-1	+1	-1	-1
9	-1	-1	-1	+1	-1	+1	+1
10	+1	-1	-1	+1	+1	+1	-1
11	-1	+1	-1	+1	+1	-1	+1
12	+1	+1	-1	+1	-1	-1	-1
13	-1	-1	+1	+1	+1	-1	-1
14	+1	-1	+1	+1	-1	-1	+1
15	-1	+1	+1	+1	-1	+1	-1
16	+1	+1	+1	+1	+1	+1	+1

Under a customized control program for powder layering experiments, powder layers were built to a total bed depth of 12.7 mm, with a corresponding volume of 102.87 ml. Samples were weighed on a digital balance.

A convenient way of summarizing the data of such a design is to express the results in terms of main effects. The main effect of a factor X is the average of all occurrences where X is high minus the average of all occurrences where X is low [consult Montgomery for details]. Figures A1 and A2 display the differences in output caused by the two levels of each input variable, for two sample powders. Each line segment is centered about the grand mean. For each pair of points and the corresponding control factor, the higher one is calculated as the grand mean plus half the main effect, and the lower is the grand mean minus half the main effect.

Figure A1. Layered Packing Density Main Effects for Alumina 30 μm

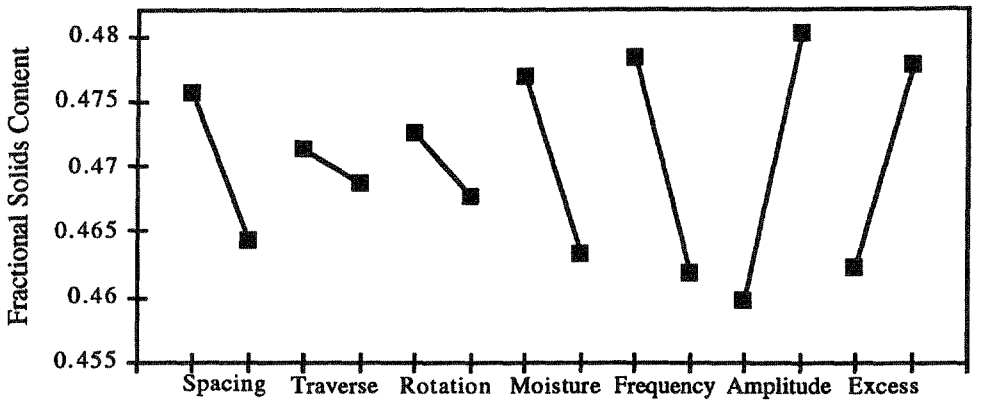

Figure A2. Layered Packing Density Main Effects for Alumina 10 μm

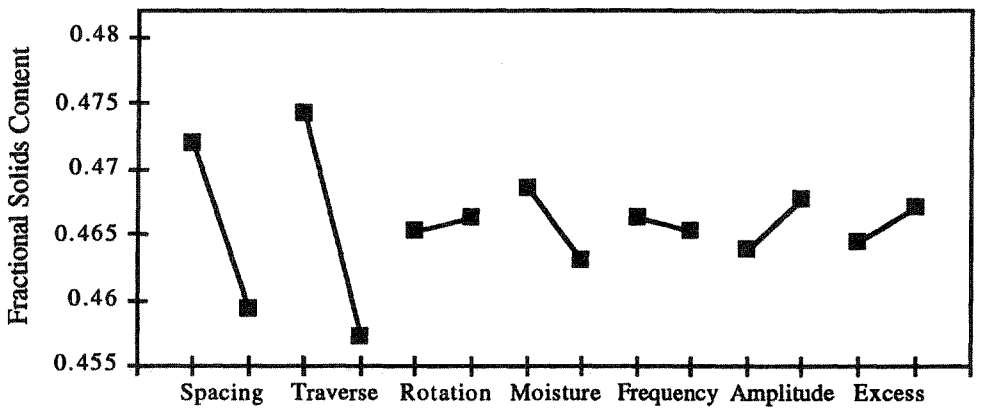

A simple verification experiment was run for the standard 3DP powder (30 μm alumina), using the main effects that predicted highest density. FSC values were 0.520 and 0.521, for an average of 0.521, higher than all values in the experimental design array.